Static and Dynamic Analysis of a 200 m High Concrete Faced Dam Based on a Generalized plasticity Model

Xu Bin
The State Key Laboratory of Coastal and Offshore Engineering, Dalian University of Technology, Dalian, 116024

Zou Degao
The State Key Laboratory of Coastal and Offshore Engineering, Dalian University of Technology, Dalian, 116024

Kong Xianjing
The State Key Laboratory of Coastal and Offshore Engineering, Dalian University of Technology, Dalian, 116024

SUMMARY:
Concrete face rockfill dams (CFRDs) are becoming a widely used type of rockfill dam in China. In many cases, the design and construction of CFRDs are based primarily on precedent and engineering judgments. Few numerical or analytical methods have been developed to properly evaluate the deformation of CFRDs, which is important for dam safety and for subsequent evaluation of seismic performance. Elastic modulus、load and unload plastic modulus of generalized plastic P-Z model were modified by considering pressure dependency of sand gravel materials. The parameters of modified model were calibrated by static and dynamic large-scale triaxial experiments of sand gravels for dam. Static and dynamic finite element method (FEM) was employed to analyze a 200 m sand gravel concrete faced rockfill dam (CFRD) by using the modified model. The results show that permanent deformation of dam can be obtained directly by using improved generalized plastic model under earthquake. The behaviours of static deformation, dynamic response and permanent deformation of dam are reasonable through elastic-plastic analysis. It is concluded that static and dynamic finite element analysis of high CFRD is feasible by using improved generalized plastic model considering pressure dependency.

Keywords: generalized plastic model; concrete faced rockfill dam, finite element analysis; dynamic response; permanent deformation.

1. GENERAL INSTRUCTIONS

Numerical simulations of CFRDs include construction, operation and earthquake period analysis. Duncan-Chang E-B model (Duncan and Chang 1970) is the most model for construction and operation analysis of CFRDs. Dynamic response analysis is an important technique for CFRDs seismic hazards simulation. The equivalent linear analysis based on viscoelastic constitutive models (Hardin 1972) is the main method used currently for the dynamic response analysis of high CFRDs. However, the equivalent linear analysis cannot be used to reasonably evaluate the seismic residual deformation of the dam, which is important for the seismic design of high CFRDs. To overcome this disadvantage, two approximate approaches are used to evaluate the seismically-induced residual deformation of embankment dams. One is the limit equilibrium method for rigid block - Newmark sliding block analysis (Newmark 1965) - based on the yield acceleration concept and the other one is the global deformation method based on the strain potential concept proposed (Serff et al. 1976). However, in the above two approaches dynamic response analysis and residual deformation calculation process are not uniform.

In the generalized plasticity theory, the yield surface and plastic potential are not explicitly defined. Instead, direction vectors are used. With appropriate formulations for the direction of plastic flow, loading–unloading directions and plastic moduli, salient behavior of soil can be described. Thus, generalized plasticity allows a less complicated simulation of experimental results for different loading conditions. This theory was introduced and applied to geomaterials (Mroz and Zienkiewicz 1984) and was developed by Pastor and Zienkiewicz (Pastor and Zienkiewicz 1990).

Recently, several improvements on the generalized plasticity model have been proposed (Pastor et al. 1993; Sassa and Sekiguchi 2001; Ling and Liu 2003; Ling and Yang 2006). In Pastor et al. (Pastor et al. 1993), anisotropy was considered, whereas in Sassa and Sekiguchi (Sassa and Sekiguchi 2001), the effects of principle stress rotation were proposed, and in Ling et al. (Ling and Liu 2003; Ling and Yang 2006), the pressure-level dependency and the critical state concept were adopted, respectively.
In this paper, based on the work of Pastor et al. (Pastor et al. 1993) and Ling and Liu (Ling and Liu 2003), the generalized plasticity model for sand was modified to better consider the pressure dependency of rockfill materials under loading, unloading and reloading conditions. The model was incorporated into a three-dimensional FEM program (Geotechnical Dynamic Nonlinear Analysis-GEODYNA). Furthermore, 2D static and dynamic numerical analyses were carried out to understand the behavior of a 200m high CFRD during construction and earthquake period.

2. CONSTITUTIVE MODEL

In this study, the modified generalized model was used for rockfill materials and a perfect elasto-plastic interface model depending pressure level was employed for interface between the concrete slab and the cushion gravel. Detailed describe of the constitutive models for rockfills are referred as Appendix A (Xu et al. 2012). The interface model is introduced as following:

Goodman contact elements (Goodman et al. 1968) with zero thickness, as shown in Figure 2, were applied between face slabs and rockfills. Same elements were also applied for simulating slabs joints and peripheral joints. The relationship between force and displacement of contact element is expressed as:

$$\begin{Bmatrix} \Delta F_{xy} \\ \Delta F_{yy} \end{Bmatrix} = \begin{Bmatrix} k_{xy} & 0 \\ 0 & k_{yy} \end{Bmatrix} \begin{Bmatrix} \Delta \delta_{xy} \\ \Delta \delta_{yy} \end{Bmatrix} \tag{2.1}$$

Where, ΔF_{yx} is the incremental shear stresses, k_{yx} is the shear stiffness, and $\Delta \delta_{yx}$ is the incremental shear displacements in the shear direction. ΔF_{yy} is incremental normal stress, k_{yy} is the normal stiffness and $\Delta \delta_{yy}$ is the incremental normal displacement.

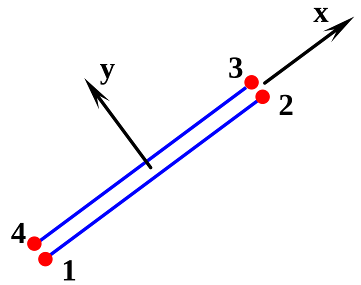

Figure 2. Sketch diagram of a Goodman element

The perfect elasto-plastic interface model depending pressure level was used for interface between face slabs and rockfills for construction and seismic response analysis. The stiffness in the tangent and normal directions of the 2-D contact element can be expressed as:

$$k_{yx} = k_1 p_a \left(\frac{\sigma_y}{p_a} \right)^n \qquad \tau_{yx} < \mathrm{c} + \sigma_z \mathrm{tg}\varphi \tag{2.2}$$

$$k_{yx} = 0 \qquad \tau_{yx} > \mathrm{c} + \sigma_z \mathrm{tg}\varphi$$

$$k_{yy} = k_2 \qquad \text{under compression} \tag{2.3}$$

$$k_{yy} = 0 \qquad \text{under tension} \tag{2.4}$$

where p_a is the atmospheric pressure; k_{yx} is the tangential coefficients of shear stiffness in the shear direction; k_1 is the contact surface modulus factor; n is the contact surface modulus exponent; R_f is the failure ratio; φ is the internal friction angle of the contact surface; σ_y is the normal stress; τ_{zx} and τ_{zy} are the shear stresses, and c is the interface cohesion; k_2 is the compressive stiffness.

3. PARAMETERS IDENTIFICATION

3.1. Slabs

Linear elastic model was used to simulate the concrete face slabs. According to the design information of the concrete face slabs, the detailed parameters were taken as density ρ = 2.40 g/cm^3, elastic modulus E = 28000 MPa and Passion's ratio v = 0.167.

3.2. Rockfill Materials

The maximum particle size of the rockfill materials is 800 mm, and it was impossible to calibrate the model parameters using element tests, such as triaxial tests, on the actual materials. In this study, the parallel gradation technique was used to obtain rockfill that had the same rock origin but smaller particles. A total of seventeen parameters are required for the modified generalized plasticity model. A group of monotonic and cyclic triaxial tests are carried out using the sand gravel materials of a CFRD. The parameters are given in Table 3.1. Figures 2-4 compare the results given by experimental tests and those by numerical simulations. It can be seen that the numerical results agree well with the experimental results under monotonic and cyclic loadings. It can be concluded that the parameters for the modified generalized plastic model are reasonable.

Table 3.1. Parameters of gravels

G_0	K_0	M_g	M_f	α_f	α_g	H_0	H_{U0}	m_s
800	2400	1.65	1.6	0.3	0.3	350	2e7	0.5
m_v	m_l	m_u	r_d	γ_{DM}	γ_u	β_0	β_1	
0.5	0.5	1	20	70	30	100	0.03	

3.3. Interface

The interface between the concrete slab and the cushion gravel of a CFRD was experimentally studied by Zhang and Zhang (Zhang and Zhang 2008). Based on the tests results, the parameters of the perfect elasto-plastic interface model were determined and listed in Table 3.2.

Table 3.2. Parameters of interface

k_1	k_2	n	φ	c /MPa
300	1e10	0.8	41.5	0

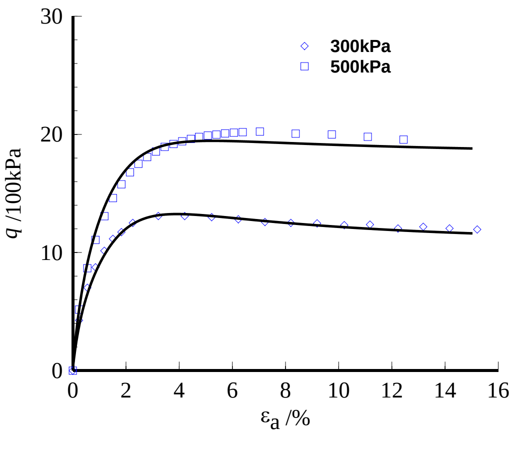

Figure 2. Static stress-strain curve of gravel material

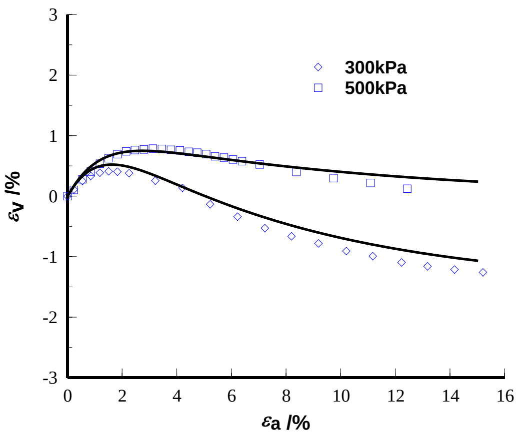

Figure 3. Static volumetric strain-axial strain curve of gravel material

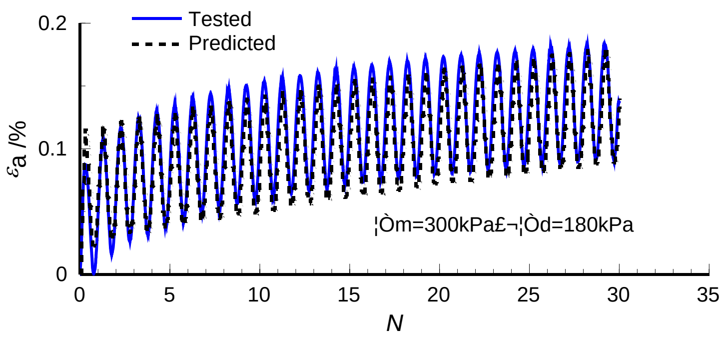

(a) Axial strain

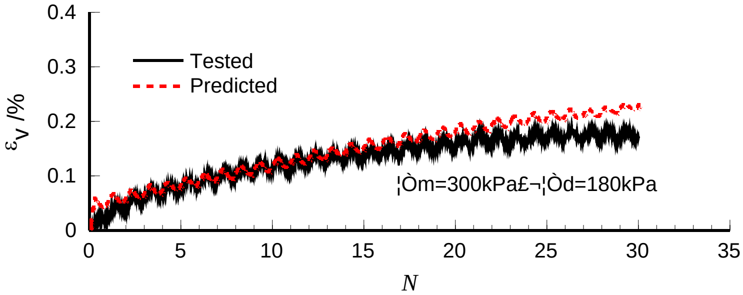

(b) Volumetric strain

Figure 4. Axial and volumetric strain time history curve of permanent deformation test of gravel material

4. FE ANALYSIS

4.1. FE Mesh

The basic features of the CFR dam are outlined herein with the help of Figure 5, which shows a cross-section and some characteristic details of a typical design. The main body of the CFR dam consists of sand gravels. The sand gravel materials and slabs are simulated by Quadratic elements. The thickness of each layer is less than 8 m. The bottom boundary of the dam is fixed at x and y direction. The water pressure is simulated as surface force on the slabs.

4.2. Input ground motions

The input acceleration time histories are shown in Figures 6 and 7. The PGA of horizontal direction on the bedrock of the dam is 0.30g, and the vertical one is assumed to be 2/3 of the horizontal.

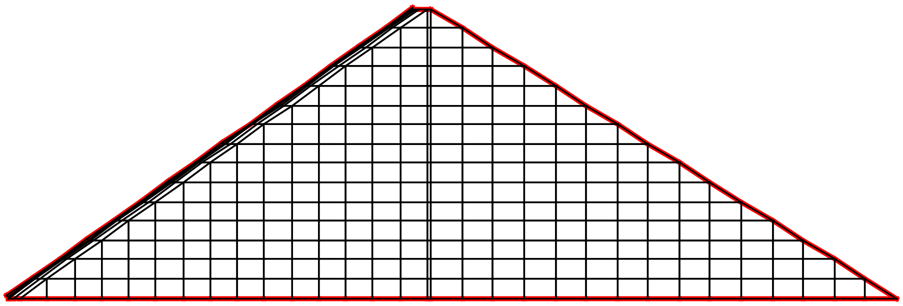

Figure 5. FEM mesh of dam calculated

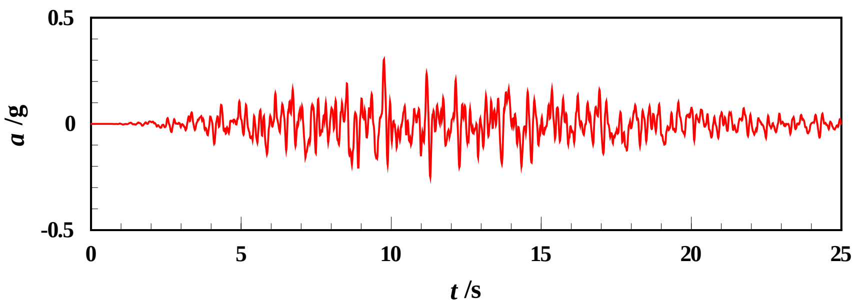

Figure 6. Horizontal seismic acceleration time history by site spectrum of CFRD

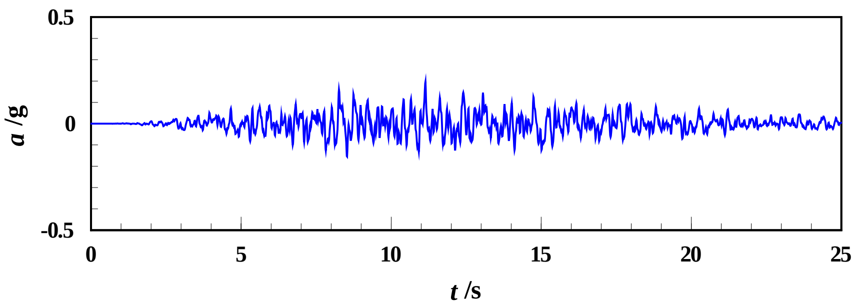

Figure 7. Vertical seismic acceleration time history by site spectrum of CFRD

4.3. Damping

Similar to other hysteresis models for soils, the generalized plasticity model can capture the material damping at finite strain but predicts much smaller damping than that of actual soils at infinitesimal strain. Rayleigh damping was used to compensate for this deficiency. A viscous damping ratio of 5% was assumed for the rockfill materials 0. The same damping ratio was also assumed for the concrete slabs.

5. RESULTS AND ANALYSIS

Firstly, static analysis was carried out to simulate the process of dam construction and water storage. Secondly, dynamic analysis was performed, in which the dynamic water pressure was simulated by adding mass method (Westergaard 1933).

5.1. Construction Process Simulation

Figures 7-10 show the contours of the principle stress and displacement of the dam at the end of construction and full impoundment. At the end of construction, the major and minor principle stress is 3.0MPa and 1.5 MPa, respectively. The horizontal displacement is 0.40 m to upstream and 0.26 m to downstream. The settlement reaches 0.83 m. After full impoundment, the major and minor principle stress increases to 3.4 MPa and 1.7 MPa, due to the effects of water pressure. Also, the horizontal displacement varies to downstream. The simulated results are according with the regular pattern of CFRDs.

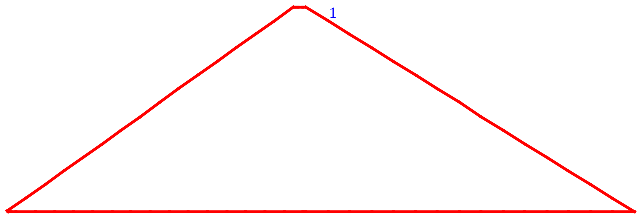

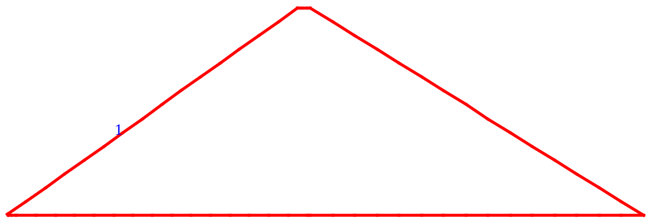
1


1

This research was supported by National Natural Science Foundation of China (No. 51138001, 90815024, 50908032) and the Fundamental Research Funds for the Central Universities of China (No. DUT11ZD110, DUT12LK37). The supports are gratefully acknowledged.

APPENDIX A:

Generalized plasticity model for sand (Pastor, 1990)

In plasticity theory, the strain increment can be decomposed into two parts

$$\mathrm{d}\boldsymbol{\varepsilon} = \mathrm{d}\boldsymbol{\varepsilon}^{\mathrm{e}} + \mathrm{d}\boldsymbol{\varepsilon}^{\mathrm{p}} \tag{A.1}$$

where $\mathrm{d}\boldsymbol{\varepsilon}^{\mathrm{e}}$ is incremental elastic strain tensor, and $\mathrm{d}\boldsymbol{\varepsilon}^{\mathrm{p}}$ is incremental plastic strain tensor.

The stress-strain relationship is expressed as:

$$\mathrm{d}\boldsymbol{\sigma}^{'} = \mathbf{D}^{\mathrm{ep}} : \mathrm{d}\boldsymbol{\varepsilon} \tag{A.2}$$

In generalized plasticity theory, the elasto-plastic stiffness tensor is expressed as:

$$\mathbf{D}^{\mathrm{ep}} = \mathbf{D}^{\mathrm{e}} - \frac{\mathbf{D}^{\mathrm{e}} : \mathbf{n}_{\mathrm{g}} : \mathbf{n}^{\mathrm{T}} : \mathbf{D}^{\mathrm{e}}}{H + \mathbf{n}^{\mathrm{T}} : \mathbf{D}^{\mathrm{e}} : \mathbf{n}_{\mathrm{g}}} \tag{A.3}$$

where

$\mathrm{d}\boldsymbol{\sigma}^{'}$: incremental effective stress tensor

$\mathrm{d}\boldsymbol{\varepsilon}$: incremental strain tensor

$\mathbf{D}^{\mathrm{ep}}$: elasto-plastic stiffness tensor

$\mathbf{D}^{\mathrm{e}}$: elastic stiffness tensor

$\mathbf{n}$: loading direction vector

$\mathbf{n}_{g}$: flow direction vector

H : plastic modulus

The distinction between loading and unloading directions is described through the following criteria:

$$\mathbf{n} : \mathrm{d}\boldsymbol{\sigma}^{\mathrm{e}} > 0 \quad \text{(loading)} \tag{A.4a}$$

$$\mathbf{n} : \mathrm{d}\boldsymbol{\sigma}^{\mathrm{e}} < 0 \quad \text{(unloading)} \tag{A.4b}$$

where $\mathrm{d}\boldsymbol{\sigma}^{e}$ is the elastic stress increment.

The following generalized expression is proposed for the stress-dilatancy relationship (Nova, 1982):

$$d_g = \frac{d\varepsilon_v^p}{d\varepsilon_s^p} = \left(1 + \alpha_g\right)\left(M_g - \eta\right) \tag{A.5}$$

where $d\varepsilon_v^p$ and $d\varepsilon_s^p$ are the incremental plastic volumetric and deviatoric strains, respectively. M_g is the slope of the critical state line in the $p^{'} - q$ plane, $\eta = q / p^{'}$ is the stress ratio, and α_g is a model parameter.

M_g is related to the angle of internal friction at the critical state $\phi_g^{'}$ and Lode's angle θ following the smoothed Mohr-Coulomb criterion proposed by Zienkiwicz and Pande (Zienkiewicz, 1977):

$$M_g = \frac{6 \sin \phi_g^{'}}{3 - \sin \phi_g^{'} \sin 3\theta} \tag{A.6}$$

The flow direction vector in triaxial space is then defined as:

$$\mathbf{n}_g^T = \left(n_{gv}, n_{gs}\right)$$

with $n_{gv} = d_g / \sqrt{(1 + d_g^2}$ and $n_{gs} = 1 / \sqrt{(1 + d_g^2}$.

Non-associated flow rule is assumed in the model and the loading direction vector is defined as:

$$\mathbf{n}^T = (n_v, n_s)$$

with $n_v = d_f / \sqrt{(1+d_f^2}$, $n_s = 1/\sqrt{(1+d_f^2}$ and $d_f = (1+\alpha_f)(M_f - \eta)$. Here M_f and α_f are both model parameters.

The elastic behavior is defined by the shear and bulk moduli:

$$K = K_0 \frac{p'}{p'_0} \tag{A.7}$$

$$G = G_0 \frac{p'}{p'_0} \tag{A.8}$$

Where K_0、G_0 are the elastic volumentric and shear moduli respectively, p' is the mean effective stress, and p'_0 is a reference value.

The plastic modulus under loading and reloading is defined as:

$$H_L = H_0 \cdot p' \cdot H_f \cdot (H_v + H_s) \cdot H_{DM} \tag{A.9}$$

$$H_f = \left(1 - \eta/\eta_f\right)^4 \tag{A.10}$$

$$\eta_f = \left(1 + 1/\alpha_f\right) M_f \tag{A.11}$$

$$H_v = 1 - \eta/M_g \tag{A.12}$$

$$H_s = \beta_0 \beta_1 \exp(-\beta_0 \xi) \tag{A.13}$$

$$H_{DM} = \left(\frac{\varsigma_{\max}}{\varsigma}\right)^{\gamma_{DM}} \tag{A.14}$$

$$\varsigma = p' \cdot \left[1 - \left(\frac{1+\alpha_f}{\alpha_f}\right) \cdot \frac{\eta}{M_f}\right]^{1/\alpha_f} \tag{A.15}$$

where H_0 is the plastic modulus number; H_f , H_v , and H_s are plastic coefficients; $\xi = \int \left| d\varepsilon_s^q \right|$ is the accumulative plastic strain; and β_0 、 β_1 、 and γ_{DM} are model parameters.

The plastic modulus under unloading is defined as:

$$H_u = H_{u0} \left(\eta_u/M_g\right)^{-\gamma_u} \qquad \left|\eta_u/M_g\right| < 1 \tag{A.16}$$

$$H_u = H_{u0} \qquad \left|\eta_u/M_g\right| \geq 1 \tag{A.17}$$

Generalized plasticity model modified for rockfills (Xu et al. 2012)

The original model was mainly used for sand liquefaction analysis with small effective confining pressure. However, the confining pressure varies from 0 to 3 MPa for high rockfill dams. In this paper, to better consider the wide range of the confining pressure and the associated particle crushing on the response of rockfills in the dam, which differs from that of sandy liquefaction problem, Equations (A.7-9 and A.16) were modified as:

$$K = K_0 p_a (p'/p_a)^{m_v} \tag{A.18}$$

$$G = G_0 p_a (p'/p_a)^{m_s} \tag{A.19}$$

$$H_L = H_0 \cdot p_a \cdot \left(p'/p_a\right)^{m_l} \cdot H_f \cdot (H_v + H_s) \cdot H_{DM} \cdot H_{den} \tag{A.20}$$

$$H_u = H_{u0} \cdot p_a \cdot \left(p'/p_a\right)^{m_u} \cdot \left(\eta_u/M_g\right)^{-\gamma_u} \cdot H_{den} \qquad \left|\eta_u/M_g\right| < 1 \tag{A.20}$$

Where pa is the atmospheric pressure (equals to 100 kPa); H_{DM} is also modified as $e^{(1-\eta/\eta_{\max})*\gamma_{DM}}$ in this study; $\eta_{\max}$ is the largest value of the stress ratio ever reached; $H_{den} = \exp(-\gamma_d \varepsilon_v)$ is the densification coefficient, which takes into account the effects of cyclic hardening as proposed in Ling and Liu (Ling and Liu, 2003).

All of the exponents for K, G, H_L, and H_u were defined as 0.5 for sandy soils in Ling and Liu (Ling and

Liu, 2003), which may not be appropriate for rockfills. In particular, rockfill materials exhibit considerable particle crushing under modest confining pressure and shear stress while most sandy soil particles are much less crushable.

REFERENCES

Duncan J M, and Chang C Y. (1970). Nonlinear Analysis of Stress and Strain in Soils. *Journal of the Soil Mechanics and Foundation Division* **96:SM5**,1629-1653.

Hardin B. O., Drnevich V. (1972). Shear modulus and damping in soils. *Journal of Soil Mechanics and Foundation Division* **98:7**, 667-692.

Newmark. N. M. (1965). Effects of earthquakes on dams and embankments. *Geotechnique* **15:2**, 139-160.

Serff, N., Seed, H. B., Makdisi, F. I., and Chang, C. K. (1976). Earthquake Induced Deformations of Earth Dams. *Report No. EERC/76 -4, Earthquake Engineering Research Center*, University of California, Berkeley

Mroz Z., Zienkiewicz O. C. (1984). Uniform formulation of constitutive equations for clay and sand. *Mechanics of engineering materials*, C. S. Desai, R. H. Gallangher. New York, Wiley, 415-450.

Pastor M., Zienkiewicz O. C. (1990). Generalized plasticity and the modeling of soil behavior. *Int. J. Numer. Analyt. Meth. Geomech.*, **14:3**, 151-190.

Pastor M., Zienkiewicz O. C., Xu G. D. et al. (1993). Modeling of sand behavior: Cyclic loading, anisotropy and localization. *Modern approaches to plasticity*, D. Kolymbas. New York, Elsevier, 469-492.

Sassa S., Sekiguchi H. (2001). Analysis of waved-induced liquefaction of sand beds. *Geotechnique*, **51:2,** 115-126.

Ling H. I., Liu H. (2003). Pressure dependancy and densification behavior of sand through a generalized plasticity model. *Journal of Engineering Mechanics, ASCE*, **129:8**, 851-860.

Ling H. I., Yang S. (2006). Unified sand model based on the critical state and generalized plasticity. *Journal of Engineering Mechanics, ASCE*, **132:12**, 1380-1391.

Xu B, Zou Degao, Liu Huabei. (2012). Three-dimensional simulation of the construction process of the Zipingpu concrete face rockfill dam based on a generalized plasticity model. *Comput Geotech*, **43:6**, 143-154.

Goodman R.E., Taylor R.L., Brekke T.L. (1968). A model for the mechanics of jointed rock. *J Soil Mech Found Div, ASCE*, **94:SM3**, 637-659.

Zhang G, Zhang J.M. (2008). Unified modeling of monotonic and cyclic behavior of interface between structure and gravelly soil. *Soils and Foundation*, **48:2**, 237-251.

Westergaard H. M. (1933). Water pressures on dams during earthquakes. *Trans. ASCE*, 98: 418-433.

Alemdar Bayraktar (2010). Murat Emre Kartal. Linear and nonlinear response of concrete slab on CFR dam during earthquake. *Soil Dynamics and Earthquake Engineering*, **30:10**, 990-1003.

Pastor M., Zienkiewicz O. C. (1990). Generalized plasticity and the modeling of soil behavior. Int. J. Numer. Analyt. Meth. Geomech., **14:3**, 151-190.

Nova, R. (1982). A constitutive model under monotonic and cyclic loading. *In Soil mechanics-transient and cyclic loads*. Edited by G. Pande and O.C. Zienkiewicz. John Wiley & Sons, Ltd., New York, 343–373.

Zienkiewicz O. C., and Pande, G. N. (1977). Some useful forms of isotropic yield surface for soil and rock mechanics. *Finite Elements in Geomechanics*, G. Gudehus, eds., Wiley, New York, 179-190.

Ling H. I., Liu H. (2003). Pressure dependancy and densification behavior of sand through a generalized plasticity model. *Journal of Engineering Mechanics*, ASCE, **129:8**, 851-860.